2012 IEEE/RSJ International Conference on
Intelligent Robots and Systems
October 7-12, 2012. Vilamoura, Algarve, Portugal

Feedback Control of Many Differential-Drive Robots with Uniform Control Inputs

Aaron Becker, Cem Onyuksel, Timothy Bretl

***Abstract*— In this paper, we derive a globally asymptotically stabilizing feedback control policy for a collection of differential-drive robots under the constraint that every robot receives exactly the same control inputs. We begin by assuming that each robot has a slightly different wheel size, which scales its forward speed and turning rate by a constant that can be found by offline or online calibration. The resulting feedback policy is easy to implement, is robust to standard models of noise, and scales to an arbitrary number (even a continuous ensemble) of robots. We validate this policy with hardware experiments, which additionally reveal that our feedback policy still works when the wheel sizes are unknown and even when the wheel sizes are all approximately identical. These results have possible future application to control of micro- and nano-scale robotic systems, which are often subject to similar constraints.**

I. Introduction

Next-generation micro-scale and nano-scale robotic systems have little-to-no onboard computation, and most are controlled by global signals, where all robots in the system receive uniform control inputs. Examples include the magnetic micro/nano robots of Nelson et al. [1], [2] and Sitti et al. [3], [4], the electric-field controlled paramecium studied by Hasegawa et al. [5], the electrokinetic and optically controlled bacteria demonstrated by Pappas et al. [6], and the magnetic-field controlled bacteria demonstrated by Martel et al. [7] and Julius et al. [8].

This paper focuses on robotic systems that can be modeled as nonholonomic unicycles. Two such systems are shown in Fig. 1: light-driven nanocars and scratch-drive micro-robots.

The light-driven nanocar [9], [10] is a synthesized molecule $1.7\times1.38n$m in size containing a uni-directional molecular motor, actuated by a certain wavelength of light. Future work by Tour et al. aims to add controllable steering to this molecule.

The scratch-drive micro-robot, from Donald and Paprotny et al. [11], [12] is a device $60\times250\mu$m in size actuated by varying the electric potential across a substrate; multiple scratch-drive robots on the same substrate are controlled by this single uniform control input. To independently control each micro-robot, the system is designed with unique robots such that individual robots can be actuated while the others are immobilized or spin in place.

The motion of both systems can be roughly approximated by a nonholonomic unicycle. A common question is therefore—how do we steer a collection of unicycles under the constraint that every one receives exactly the same control inputs? This question is the one we address here.

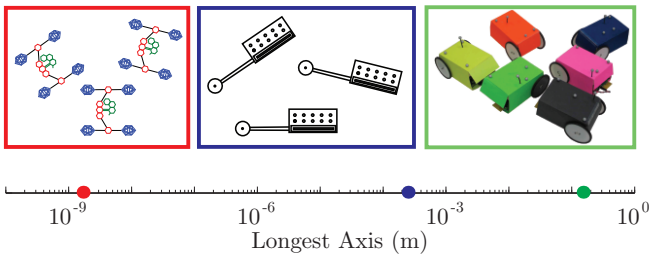

Fig. 1. Three robotic systems with uniform inputs. On the left, three light-driven nanocars [10]. In the middle, three scratch-drive micro-robots [12]. On the right, six differential-drive robots.

As a case study, we will look at a collection of differential-drive robots under this same constraint—that every robot receives exactly the same control inputs. Nominally, this system is not controllable. The path followed by each robot will be a rigid-body transformation of the path followed by every other robot. In practice, however, each robot is slightly different, and this inhomogeneity can be exploited in a systematic way in order to recover controllability. In particular, we will show that if each robot has a different wheel size, then we can derive a globally asymptotically stabilizing feedback control policy that steers the position of all robots (independently) between given start and goal configurations, despite the fact that they all receive the same control inputs. Similar inhomogeneities can be found in the systems of Fig. 1 (and in other micro/nano-scale robotic systems). For example, small imperfections in their scratch-drive actuators lead to speed variations between different scratch-drive micro-robots.

Our approach is based on the application of ensemble control, which we used in previous work to derive an approximate (open-loop) steering algorithm for a nonholonomic unicycle despite model perturbation (e.g., unknown wheel size) that scales both the forward speed and turning rate by an unknown but bounded constant [13]. Rather than steer one unicycle with an unknown parameter, we chose to steer an infinite collection of unicycles, each with a particular value of this parameter in some bounded set. Following the terminology introduced by [14]–[17], we called this fictitious collection of unicycles an *ensemble* and called our approach to steering *ensemble control*. The idea was that if the same control inputs steered the entire ensemble from start to goal, then surely they would steer the particular unicycle of interest from start to goal, regardless of its wheel size.

Here, we take advantage of this idea in a slightly different way. Rather than trying to mitigate the effects of bounded

A. Becker and C. Onyuksel are with the Department of Electrical and Computer Engineering; T. Bretl is with the Department of Aerospace Engineering, University of Illinois at Urbana-Champaign, Urbana, IL, 61801, USA {abecker5,conyuks2,tbretl}@illinois.edu

model perturbation (i.e., of inhomogeneity), we are trying to exaggerate these effects. Basic controllability results carry over from our previous work. Our main contribution in this paper is to derive a closed-loop feedback policy that guarantees exact asymptotic convergence of the ensemble to any given position. We note that, for single robots, it is possible to build a robust feedback controller that regulates position and orientation [18]. It is not obvious that the same can be done for an infinite collection of robots.

Our paper proceeds as follows. In Section II, we provide a globally asymptotically stabilizing feedback control policy to control an ensemble of differential-drive robots. We discuss implementation details in Section III. We demonstrate the convergence of our policy under a standard noise model in simulation (Section IV) and in hardware experiments (Section V). These experiments revealed surprising results: *1)* our policy still works when the parameter values are incorrectly specified and *2)* our policy still works when all robots are approximately identical with certain levels of process noise. We conclude in Section VI.

II. Globally Asymptotic Stabilization of An Ensemble of Unicycles

In this section, we provide a control policy that globally asymptotically stabilizes an infinite ensemble of unicycles. This control policy sets the linear velocity $u_1(t)$ to decrease the position error. There exist configurations at which no $u_1(t)$ can decrease the position error; however, we prove that at any such configuration, except the origin, the ensemble can always be rotated in place until there exists some $u_1(t)$ that will decrease the position error.

Consider a single unicycle that rolls without slipping. We describe its configuration by $q = [x, y, \theta]^\top$ and its configuration space by $\mathcal{Q} = \mathbb{R}^2 \times \mathbb{S}^1$. The control inputs are the forward speed $u_1 \in \mathbb{R}$ and turning rate $u_2 \in \mathbb{R}$. The kinematics of the unicycle are given by

$$\dot{q}(t) = u_1(t) \begin{bmatrix} \cos\theta \\ \sin\theta \\ 0 \end{bmatrix} + u_2(t) \begin{bmatrix} 0 \\ 0 \\ 1 \end{bmatrix}. \tag{1}$$

Given $q(0), q_{\text{goal}} \in \mathcal{Q}$, the control problem for regulating position is to find inputs $u_1(t)$ and $u_2(t)$ such that for any $q(0)$ and q_{goal},

$$\lim_{t\to\infty} \left\| \begin{bmatrix} q_1(t) \\ q_2(t) \end{bmatrix} - \begin{bmatrix} q_{\text{goal},}1(t) \\ q_{\text{goal},}2(t) \end{bmatrix} \right\|_2 = 0.$$

If such inputs always exist, then we say that the system is *globally asymptotically stabilizable*.

We will solve this control problem under model perturbations which scale u_1 and u_2 by some unknown, bounded constant $\epsilon \in [1-\delta, 1+\delta]$ for some $0 \leq \delta < 1$ so that $\epsilon > 0$. On a differential-drive robot, ϵ can be mapped to wheel size.

As in [13], our approach is to steer an uncountably infinite collection of unicycles parametrized by ϵ, each one governed by

$$\dot{q}(t,\epsilon) = \epsilon \left(u_1(t) \begin{bmatrix} \cos\theta \\ \sin\theta \\ 0 \end{bmatrix} + u_2(t) \begin{bmatrix} 0 \\ 0 \\ 1 \end{bmatrix} \right). \tag{2}$$

We choose $u_2(t) = 1$ so that

$$\begin{aligned} \dot{x}(t,\epsilon) &= \epsilon u_1(t)\cos(\epsilon t) \\ \dot{y}(t,\epsilon) &= \epsilon u_1(t)\sin(\epsilon t). \end{aligned} \tag{3}$$

Theorem 1: The ensemble (3) for $\epsilon \in [1-\delta, 1+\delta]$ with $0 \leq \delta < 1$ is globally asymptotically stabilizable.

Proof: We will prove the origin is globally asymptotically stabilizable by using a control-Lyapunov function [19]. A suitable Lyapunov function is the mean squared distance of the ensemble from the origin:

$$V(t,x,y) = \int_{1-\delta}^{1+\delta} \frac{1}{2\epsilon} \left(x^2(t,\epsilon) + y^2(t,\epsilon) \right) d\epsilon \tag{4}$$

$$\begin{aligned} \dot{V}(t,x,y) &= \int_{1-\delta}^{1+\delta} \frac{1}{\epsilon} \left(x(t,\epsilon)\dot{x}(t,\epsilon) + y(t,\epsilon)\dot{y}(t,\epsilon) \right) d\epsilon \\ &= u_1(t) \int_{1-\delta}^{1+\delta} \left(x(t,\epsilon)\cos(\epsilon t) + y(t,\epsilon)\sin(\epsilon t) \right) d\epsilon \\ &= u_1(t) F(t,x,y) \end{aligned}$$

Here, $F(t,x,y)$ is the integral term which is finite as long as $x(t,\epsilon)$ and $y(t,\epsilon)$ are square integrable over ϵ. To ensure $F(t,x,y)$ is square integrable we will require that the initial configurations $x(0,\epsilon)$ and $y(0,\epsilon)$ be piecewise continuous. We note here that $V(t,x,y)$ is positive definite and radially unbounded, and $V(t,x,y) \equiv 0$ only at $(x(t,\epsilon), y(t,\epsilon)) = (0,0)$.

A. Designing a Control Policy

To make $\dot{V}(t,x,y)$ negative semi-definite, we choose

$$u_1(t) = -F(t,x,y)$$

For such a $u_1(t)$,

$$\dot{V}(t,x,y) = -\left(F(t,x,y)\right)^2.$$

Note here that $\dot{V}(t,x,y) \leq 0$, but there exists a subspace of $(x(t,\epsilon), y(t,\epsilon))$ such that $\dot{V}(t,x,y) = 0$. Because $\dot{V}(t,x,y)$ is negative semi-definite, we can only claim stability, not asymptotic stability. To gain a proof of asymptotic stability, we will use an approach similar to that of Beauchard et al. [20] to extend LaSalle's invariance principle [21] to this infinite-dimensional ensemble. We will proceed by showing the invariant set contains only the origin.

B. Finding the Invariant Set

Define the set S as all configurations where no $u_1(t)$ exists that can decrease the Lyapunov function:

$$\begin{aligned} S &= \left\{ x(t,\epsilon), y(t,\epsilon) \middle| \dot{V}\left(t, x(t,\epsilon), y(t,\epsilon)\right) = 0 \right\} \\ &= \left\{ x(t,\epsilon), y(t,\epsilon) \middle| -\left(F(t,x,y)\right)^2 = 0 \right\} \\ &= \left\{ x(t,\epsilon), y(t,\epsilon) | F(t,x,y) = 0 \right\}. \end{aligned}$$

Define the time the ensemble enters S as t_0, the orientation of each robot at t_0 as $\theta_0(\epsilon)$, and $t' = t - t_0$. We then define all configurations that remain identically in S as the invariant set S_{inv}. Any configuration that enters this set will never modify its position because $u_1(t) = -F(t,x,y) = 0$ for

any configuration in S_{inv}. Therefore we can drop the time-dependence of $x(t,\epsilon)$ and $y(t,\epsilon)$:

$$S_{inv} = \left\{ x(\epsilon), y(\epsilon) \middle| \int_{1-\delta}^{1+\delta} \Big(x(\epsilon)\cos(\epsilon t' + \theta_0(\epsilon)) + y(\epsilon)\sin(\epsilon t' + \theta_0(\epsilon)) \Big) d\epsilon \equiv 0, \quad \forall t' \geq 0 \right\}.$$

We can remove $\theta_0(\epsilon)$ with the following change of coordinates

$$\begin{bmatrix} x^*(\epsilon) \\ y^*(\epsilon) \end{bmatrix} = \begin{bmatrix} \cos\big(\theta_0(\epsilon)\big) & \sin\big(\theta_0(\epsilon)\big) \\ -\sin\big(\theta_0(\epsilon)\big) & \cos\big(\theta_0(\epsilon)\big) \end{bmatrix} \begin{bmatrix} x(\epsilon) \\ y(\epsilon) \end{bmatrix},$$

giving the invariant set

$$S_{inv} = \left\{ x(\epsilon), y(\epsilon) \middle| \int_{1-\delta}^{1+\delta} \Big(x^*(\epsilon)\cos(\epsilon t') + y^*(\epsilon)\sin(\epsilon t') \Big) d\epsilon \equiv 0, \quad \forall t' \right\}.$$

We must show that no configuration except $(x(\epsilon), y(\epsilon)) \equiv (0,0)$ is in S_{inv}. We do this by applying the Fourier transform in t'.

$$\int_{1-\delta}^{1+\delta} \left(x^*(\epsilon)\cos(\epsilon t') + y^*(\epsilon)\sin(\epsilon t') \right) d\epsilon \equiv 0, \quad \forall t'$$

$$\mathcal{F}\left[\int_{1-\delta}^{1+\delta} \left(x^*(\epsilon)\cos(\epsilon t') + y^*(\epsilon)\sin(\epsilon t') \right) d\epsilon \right] \{\omega\} \equiv 0, \quad \forall \omega$$

By linearity of the Fourier transformation this is

$$\int_{1-\delta}^{1+\delta} \Big(\mathcal{F}\left[x^*(\epsilon)\cos(\epsilon t') \right] \{\omega\} + \mathcal{F}\left[y^*(\epsilon)\sin(\epsilon t') \right] \{\omega\} \Big) d\epsilon \equiv 0, \quad \forall \omega$$

We then apply the Fourier transform of $\sin(\cdot)$ and $\cos(\cdot)$ as follows.

$$\int_{1-\delta}^{1+\delta} \sqrt{\frac{\pi}{2}} \Big(x^*(\epsilon) \left(\underline{\delta}(-\epsilon+\omega) + \underline{\delta}(\epsilon+\omega) \right) + \mathrm{i} y^*(\epsilon) \left(\underline{\delta}(-\epsilon+\omega) - \underline{\delta}(\epsilon+\omega) \right) \Big) d\epsilon \equiv 0, \quad \forall \omega, \quad (5)$$

where $\underline{\delta}(\cdot)$ is the Dirac-delta operator. The Dirac-delta operator is non-zero only when $\epsilon = \pm\omega$. Because $\epsilon \in [1-\delta, 1+\delta]$ and $0 \leq \delta < 1$, we can integrate (5) for all $\omega \in [1-\delta, 1+\delta]$ to show that in the invariant set

$$x^*(\omega) + \mathrm{i} y^*(\omega) \equiv 0, \quad \forall \omega \in [1-\delta, 1+\delta]. \quad (6)$$

Because x^* and y^* are both real-valued, (6) reduces to

$$x(\epsilon) \equiv 0, y(\epsilon) \equiv 0, \quad \forall \epsilon \in [1-\delta, 1+\delta].$$

We have shown that V is positive-definite and radially unbounded, $\dot{V}$ is negative semi-definite, and the only invariant point where $\dot{V} = 0$ is the origin. Therefore, we conclude that under the control policy

$$\begin{aligned} u_1(t) &= -\int_{1-\delta}^{1+\delta} \left(x(\epsilon)\cos(\epsilon t) + y(\epsilon)\sin(\epsilon t) \right) d\epsilon \\ u_2(t) &= 1. \end{aligned} \quad (7)$$

the origin of the ensemble (3) is globally asymptotically stable. ■

III. Implementation

In this section, we explain extensions of our control policy to unidirectional and discrete-time, finite ensembles, and we apply a standard noise model to our ensemble. These extensions are useful for implementation of our policy.

A. Extension to Unidirectional Vehicles

Some systems, including the nanocar and scratch-drive micro-robot, have unidirectional constraints on their inputs. Our control law already uses unidirectional input for u_2. This can be extended to robots with minimum turning radius (e.g. [11], [12]) by redefining the robot center as the center of rotation. To handle linear velocity constraints, we modify (7) to be non-negative by setting $u_1(t) = \max(0, -F(t))$. In simulation and hardware experiments, the resulting unidirectional control policy converges about half as fast as the original control policy. Extending the global asymptotic stability result to unidirectional inputs is a promising avenue for future work.

B. Extension to a Discrete-Time, Finite Ensemble of Robots

Thus far we have worked in continuous time for an ensemble of robots. Many real-life applications, including the micro- and nano-robots we discussed above, involve a finite number of robots which are controlled and measured in discrete time. We call an ensemble with a finite number of robots a *finite ensemble*.

To model a finite ensemble of n robots, we redefine the kinematic model from (3) as

$$\begin{aligned} \dot{x}_i &= \epsilon_i u_1(t)\cos(\theta_i(t)) \\ \dot{y}_i &= \epsilon_i u_1(t)\sin(\theta_i(t)) \\ \dot{\theta}_i &= \epsilon_i u_2(t), \end{aligned} \quad (8)$$

and in the control policy (7), we replace the integration over ϵ with a finite sum from 1 to n:

$$\begin{aligned} u_1(t) &= -\frac{1}{n}\sum_{i=1}^{n} \left(x_i\cos(\theta_i(t)) + y_i\sin(\theta_i(t)) \right) \\ u_2(t) &= 1, \end{aligned} \quad (9)$$

where for the ith robot, ϵ_i is the variable parameter, (x_i, y_i) is the position at time t, and $\epsilon_i t$ is the orientation at time t.

Reworking the proof in Section II with summations instead of integrals proves that the only point in the invariant set is

$$(x_{t,\epsilon}, y_{t,\epsilon}) = (0,0) \quad \forall \epsilon \in [1-\delta, 1+\delta],$$

and that the finite ensemble is globally asymptotically stabilizable for particular values of ϵ, with control policy (9).

To simplify implementation, we split the control policy (9) into two stages. During even stages we command the robots

to turn in place, and during odd stages we apply a linear velocity.

$$F(k) = \frac{1}{n}\sum_{i=1}^{n}\left(x_{i,k}\cos(\theta_{i,k}) + y_{i,k}\sin(\theta_{i,k})\right)$$

$$\left[u_1(k), u_2(k)\right] = \begin{cases} \left[0, \frac{\pi}{2}\right] & k \bmod 2 = 0 \\ \left[-F(k), 0\right] & k \bmod 2 = 1 \end{cases} \quad (10)$$

To model a finite ensemble in discrete time, we convert the continuous kinematics in (8) to the following discrete kinematics under control policy (10):

$$\begin{bmatrix} x_{k+1,i} \\ y_{k+1,i} \\ \theta_{k+1,i} \end{bmatrix} = \begin{bmatrix} x_{k,i} \\ y_{k,i} \\ \theta_{k,i} \end{bmatrix} + \begin{bmatrix} \epsilon_i\cos(\theta_{k,i}) & 0 \\ \epsilon_i\sin(\theta_{k,i}) & 0 \\ 0 & \epsilon_i \end{bmatrix} \begin{bmatrix} u_1(k) \\ u_2(k) \end{bmatrix}, \quad (11)$$

for $i = 1, 2, \ldots, n$ and $k \in \mathbb{Z}$. Methods in [22] can be used to show the controllability of (11).

The control policy (10) is easy to implement, never increases the summed distance of the ensemble from the goal, and is robust to standard models of noise.

C. Applying a Standard Noise Model

To model process noise, we apply the noise model in [23, Chap. 5.4.2] by Thrun et al. This model defines each discrete-time motion as a rotation, a translation, and a second rotation. It uses the four parameters $\alpha_1, \alpha_2, \alpha_3$, and α_4 to weight the correlation of noise between rotation and translation actions. If the desired rotation, translation, and second rotation are given by $[\delta_{\text{rot1}}, \delta_{\text{trans}}, \delta_{\text{rot2}}]$, then the actual actions, after noise is applied, are given by

$$\begin{aligned} \hat{\delta}_{\text{rot1}} &= \delta_{\text{rot1}} - \text{sample}(\alpha_1\delta_{\text{rot1}}^2 + \alpha_2\delta_{\text{trans}}^2) \\ \hat{\delta}_{\text{trans}} &= \delta_{\text{trans}} - \text{sample}(\alpha_3\delta_{\text{trans}}^2 + \alpha_4\delta_{\text{rot1}}^2 + \alpha_4\delta_{\text{rot2}}^2) \\ \hat{\delta}_{\text{rot2}} &= \delta_{\text{rot2}} - \text{sample}(\alpha_1\delta_{\text{rot2}}^2 + \alpha_2\delta_{\text{trans}}^2), \end{aligned} \quad (12)$$

where $\text{sample}(\sigma^2)$ generates a random sample from the zero-centered normal distribution with variance σ^2. We use this noise model for all discrete-time simulations.

IV. Simulation Results

Here, we present our simulation methodology and results for both continuous- and discrete-time simulations.

A. Continuous Time

We implemented the finite ensemble (8) with control policy (9) in MATLAB to simulate $n = \{50, 100, 500, 1000, 2000\}$ robots in continuous time for two different test cases. For these tests $\delta = 1/2$, and $\epsilon_i = 1 - \delta + \frac{2\delta}{n}i$.

1) Point to Point: Robots are initialized to $[x_i, y_i, \theta_i] = [1, 1, 0]$ and steered to the origin. Results are shown in Fig. 2.

2) Path to Point: Robots are initialized to $\theta_i = 2\pi i/n$, $[x_i, y_i] = [\cos(\theta_i, \sin(\theta_i)]$, a circle of radius 1, and steered to the origin. Results are shown in Fig. 3.

From these simulations, we see that under our control policy, the error converges asymptotically to zero. Additionally, the Lyapunov function evolution and state trajectories for $n = 1000$ and 2000 are identical, suggesting that this level of discretization accurately represents the ensemble ($n = \infty$) kinematics.

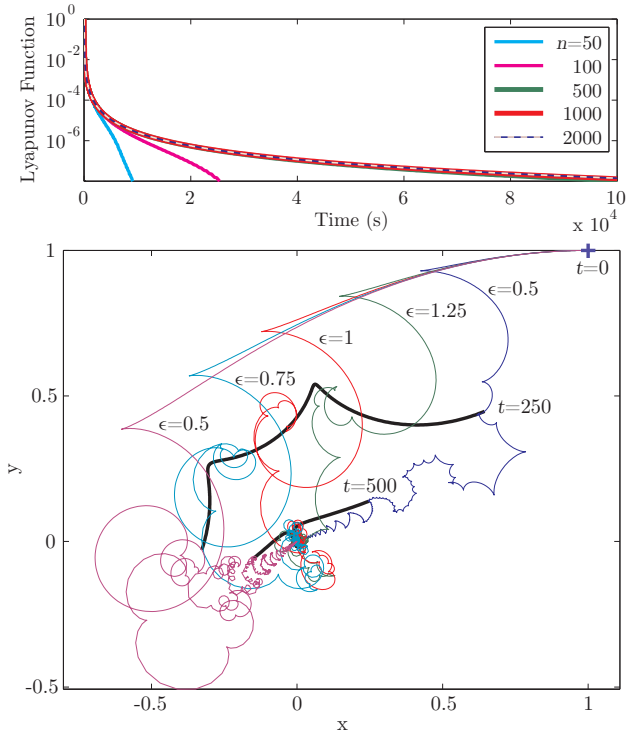

Fig. 2. Continuous time simulation of n robots, with $\epsilon \in [0.5, 1.5]$, all initialized to $(1, 1)$ and steered to $(0, 0)$ using control policy (9) and $u_2(t) = \cos(\sqrt{t})$. The simulation was run with increasing numbers of robots. SImulations with $n \geq 500$ achieved the same error, as shown in the top plot. State trajectories of the ensemble are shown in the bottom plot. Lines show the path followed for five particular values of ϵ. Thick black lines show the entire ensemble at instants of time (see video).

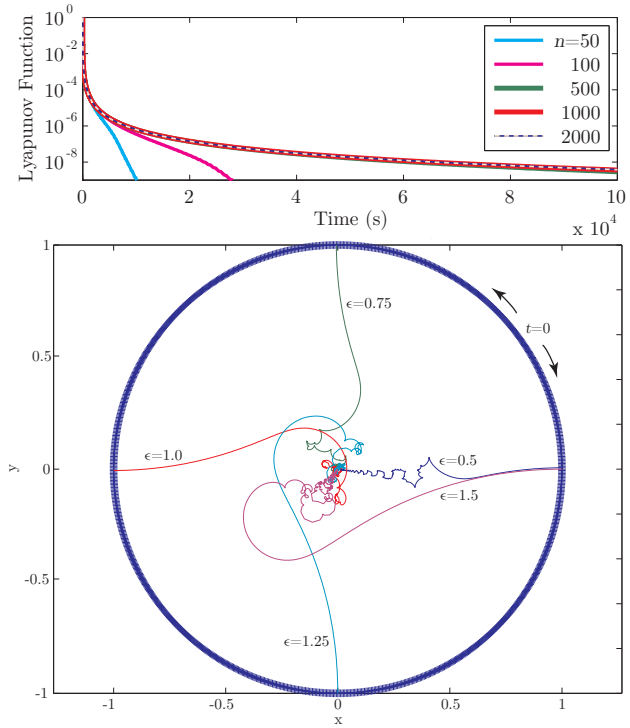

Fig. 3. Continuous time simulation of n robots, with $\epsilon \in [0.5, 1.5]$, initially evenly distributed about the unit circle and steered to $(0, 0)$ using control policy (9) and $u_2(t) = \cos(\sqrt{t})$. The simulation was run with increasing numbers of robots. Simulations with $n \geq 500$ achieved the same error, as shown in the top plot. State trajectories of the ensemble are shown in the bottom plot. Lines show the path followed for five particular values of ϵ.

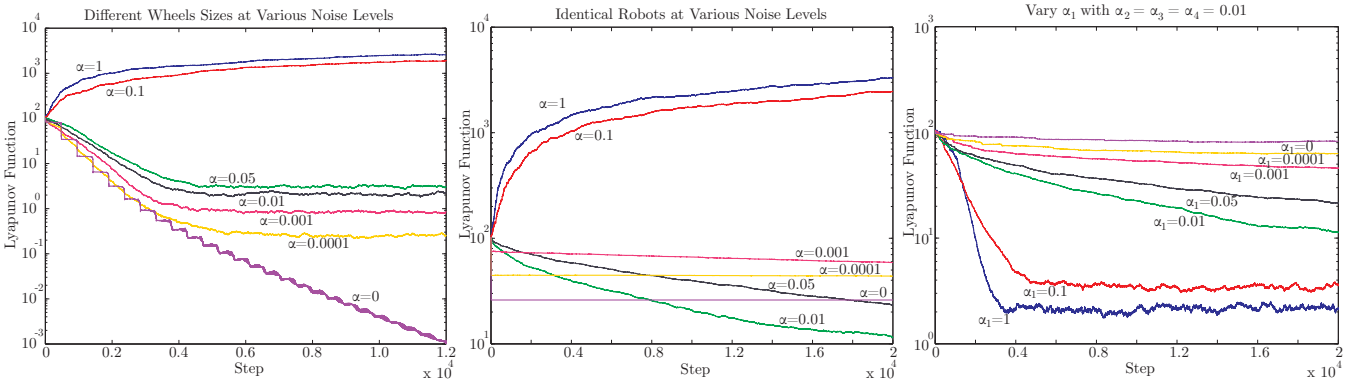

(a) (b) (c)

Fig. 4. Lyapunov function of a discrete-time, finite collection of 120 robots simulated under a standard noise model (12). 4a shows the convergence of the position error, where $\epsilon \in [0.5, 1.5]$, with different levels of noise parametrized by α; all α are equal. In 4b and 4c, all ϵ are set to 1. 4c shows that focusing the noise in the rotation (α_1) improves convergence with identical robots.

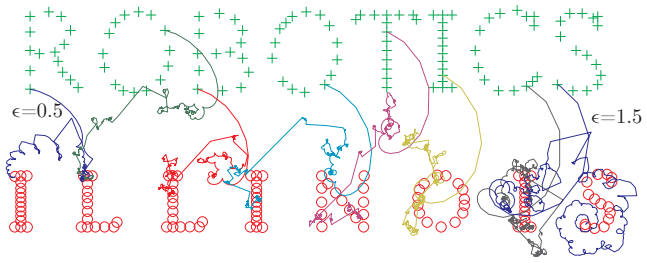

Fig. 5. Simulation results from applying the control policy from (10) for 120 robots with unicycle kinematics. Wheel size (ϵ) was evenly distributed from 0.5 to 1.5. The plot shows the the starting '+' and ending 'o' positions along with 8 selected state trajectories (see video).

B. Discrete Time

We simulated a discrete-time collection of 120 robots under various levels of process noise parameters with both differing and identical values of ϵ. Sample trajectories are shown in Fig. 5. We explored three different cases:

1) Different ϵ Values: Simulating with differing ϵ, we found that with no process noise, the position error of our robot collection converged to zero error. When the noise model (12) was applied, the error converged to a non-zero value for small values of process noise, and diverged for large values, as shown in Fig. 4a.

2) Identical Robots: When all 120 robots are identical, the smallest position error is achieved within a specific intermediate range of process noise values. Large α values caused the error to diverge, while small α values led to very slow convergence. This result is shown in Fig. 4b.

3) Effect of Rotational Noise: Again with identical robots, we held the translational and cross-term noise at 0.01, a value which converged quickly in the previous simulation, and varied the rotational noise, α_1. Convergence rate increased with α_1, up to a limit of approximately $\alpha_1 = 1$. This result is shown in Fig. 4c.

These results show that process noise is necessary for a finite collection of identical robots to be controllable. We believe this is a subset of a larger class of problems for which noise is beneficial, or even necessary, for stability and control. In particular, these results suggest that robots with uniform inputs should be designed with large rotational, but small translational and cross-term noise.

V. Hardware Experiments

Here, we describe our hardware system and explain our experimental procedures and results.

A. Differential-drive robots

Our differential robots have two large direct-drive wheels in the back, and a free-wheeling ball caster in the front, as shown in Fig. 1. In the experiments shown in this paper, we use wheels with diameters in the set $\{102, 108, 127, 152\}$mm. Trials with identical-size wheels all used 102mm wheels.

B. System Overview

Our robots are commanded to either move linearly or turn in place in units of encoder ticks. These commands are broadcast over 900MHz radio using an AeroComm 4490 card.

Four to five tracking dots are fixed to the top of each robot. Position and orientation data for each vehicle are uniquely measured by an 18-camera NaturalPoint OptiTrack system with reported sub-millimeter accuracy. A MATLAB program computes the control policy (10) and sends the global control signal.

C. Online Calibration

Calibration is not necessary for successful implementation of the controller—note that the control policies (7) and (10) do not require ϵ. In practice, the policy

$$u_1(t) = -\frac{1}{n}\sum_{i=1}^{n}\frac{1}{\epsilon_i}\left(x_i\cos(\theta_i(t)) + y_i\sin(\theta_i(t))\right)$$

with the correct ϵ values results in faster convergence. In our hardware experiments, for every translation command $u(k)$, we record beginning and ending positions to calculate d_i, the

distance traveled, and update each ϵ_i value according to the following rule

$$\epsilon_i(k+1) = \epsilon_i(k) + K\frac{|u(k)|}{M}\left(\frac{d_i}{|u(k)|} - \epsilon_i(k)\right).$$

K is the weighting we give new measurements of ϵ, and M is the maximum possible distance we may command the robot to move. For the experiments shown here $K = 0.1$ and $M = 0.7$.

D. Experiments

We conducted a series of experiments to show that our control policy converges in a real system. We show results for unique wheel sizes with online calibration, for unique wheel sizes without online calibration, and for identical wheels.

1) Unique Wheel Sizes with Online Calibration: Initially, each robot was assumed to have $\epsilon = 1$, and the actual values of ϵ were learned through online calibration. The robots were successfully commanded from a horizontal line, to a box formation, to a vertical line, and finally to a tight box formation. The results in Fig. 6 show convergence both in position and in ϵ values. Online calibration requires persistent excitation, so convergence slows as the robots approach their targets.

2) Unique Wheel Sizes without Calibration: Surprisingly, it is not necessary to know or to learn the ϵ values. For this entire experiment ϵ was set to 1. Four robots were successfully commanded from a horizontal line to a box formation, and then to a vertical line. For each formation, error converged to less than half a meter, as shown in Fig. 7.

3) Identical Wheel Sizes: Even with identical ϵ values, a collection of robots is still controllable due to process noise. Fig. 8 shows successful convergence results of four robots with identical wheel sizes commanded to the same formations as the previous experiment.

E. Applications Enabled by Position Control

The ability to control position enables many tasks. In a multimedia attachment, we demonstrate robot gathering using six robots with identical-sized wheels. Robot gathering robustly collects all the robots to one position; this primitive operation could be useful for alignment of micro- and nano-robots. To achieve robot gathering, the goal position of each robot is set to the mean position of the ensemble.

Other tasks include forming subgroups, path- and trajectory-following, dispersion, pursuit/avoidance, manipulation, and assembly. Each can be implemented by a suitable selection of time-varying target locations in (9). Simulated results for trajectory following are shown in Fig. 9.

Future work could incorporate collision and obstacle avoidance by adding a potential field to the control policy (7) as in [24, Chap. 4].

VI. Conclusion

In this paper we investigated ensembles of unicycles that share a uniform control input. Through Lyapunov analysis, we derived a globally asymptotic stabilizing controller

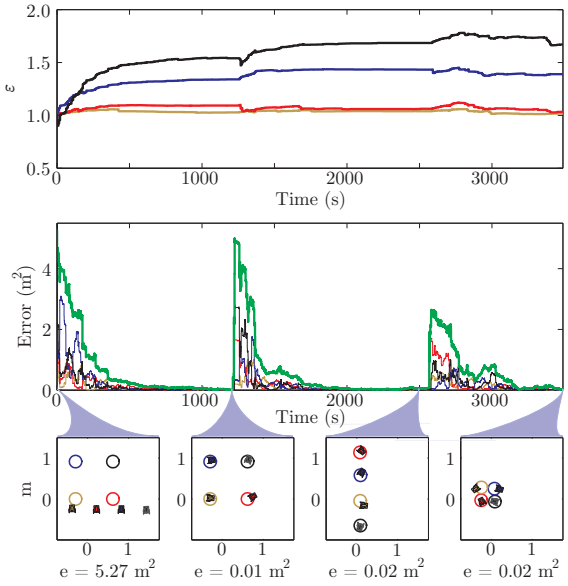

Fig. 6. Hardware experiment with unique wheel sizes and online calibration. The top plot shows ϵ values estimated by online calibration. The bottom plot shows the summed distance error as the robots were steered through the sequence of formations shown.

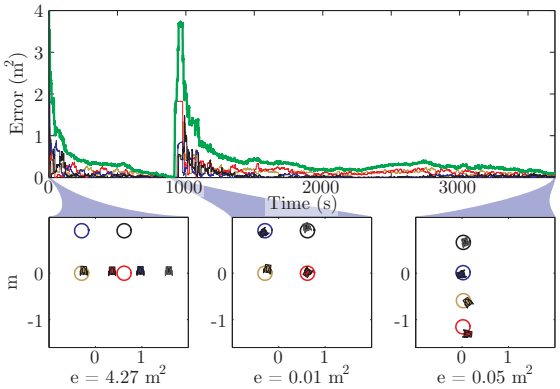

Fig. 7. Hardware experiment with unique wheel sizes and no calibration. The plot shows the summed distance error as the robots were steered through the sequence of formations shown (see video).

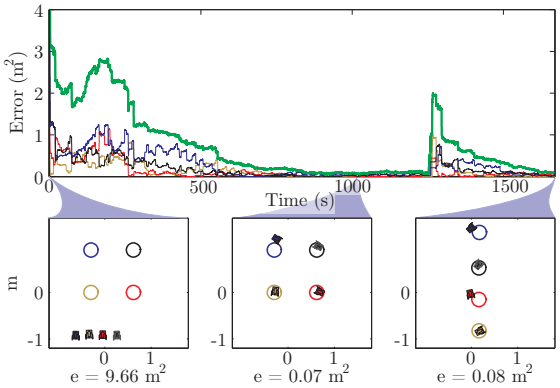

Fig. 8. Hardware experiment with identical wheel sizes. The plot shows the summed distance error as the robots were steered through the sequence of formations shown.

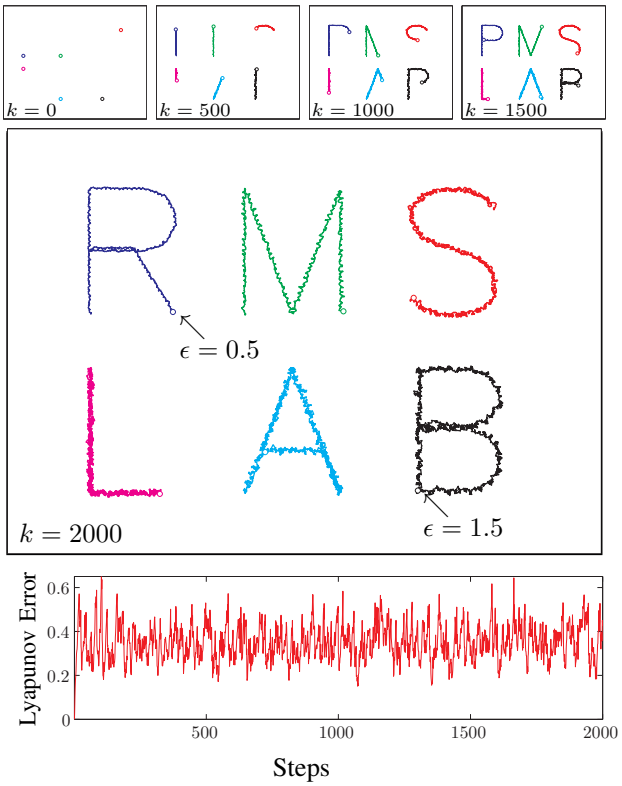

Fig. 9. Simulation of trajectory-following. Six differential-drive robots with wheel sizes ranging from 0.5 to 1.5 of nominal are steered with a common control signal to follow trajectories that spell out 'RMSLAB'. The top left robot (blue) has the smallest wheels while the lower right robot (**black**) has the largest wheels. The bottom plot shows that the Lyapunov function stabilizes around 0.37.

for a continuous-time, infinite ensemble. We extended this controller to finite collections of unicycles in continuous and discrete time. In simulation, we showed that a discrete-time, finite ensemble of unicycles converges asymptotically and rejects disturbances from a standard noise model. In hardware experiments, we demonstrated online calibration which learned the unknown parameter for each robot. These experiments led to surprising results that *1)* our controller still works when all wheel sizes are incorrectly specified and *2)* for certain levels of process noise our controller works even when all wheel sizes are the same.

This work shows that a collection of unicycles with uniform inputs to all robots can be regulated to arbitrary positions and reject disturbances from a standard noise model. If the robots have unique wheel sizes, they can converge to goals with global asymptotic stability. The analysis suggests that micro- and nano-robots with uniform inputs should be designed with large rotational, but small translational process noise.

VII. Acknowledgements

The authors thank Dan Block for his help with the hardware experiments. This work was supported by the National Science Foundation under CPS-0931871 and CMMI-0956362.

References

[1] H.-W. Tung, D. R. Frutiger, S. Panè, and B. J. Nelson, "Polymer-based wireless resonant magnetic microrobots," in *IEEE International Conference on Robotics and Automation*, May 2012, pp. 715–720.

[2] S. Schürle, K. E. Peyer, B. E. Kratochvil, and B. J. Nelson, "Holonomic 5-DOF magnetic control of 1D nanostructures," in *IEEE Int. Conf. Rob. Aut.*, May 2012, pp. 1081–1086.

[3] E. Diller, S. Floyd, C. Pawashe, and M. Sitti, "Control of multiple heterogeneous magnetic microrobots in two dimensions on nonspecialized surfaces," *IEEE Trans. Robot.*, vol. 28, no. 1, pp. 172–182, Feb. 2012.

[4] S. Floyd, E. Diller, C. Pawashe, and M. Sitti, "Control methodologies for a heterogeneous group of untethered magnetic micro-robots," *Int. J. Robot. Res.*, vol. 30, no. 13, pp. 1553–1565, Nov. 2011.

[5] T. Hasegawa, N. Ogawa, H. Oku, and M. Ishikawa, "A new framework for microrobotic control of motile cells based on high-speed tracking and focusing," in *IEEE Int. Conf. Rob. Aut.*, May 2008, pp. 3964–3969.

[6] E. B. Steager, M. Sakar, D. H. Kim, V. Kumar, and G. J. Pappas, "Electrokinetic and optical control of bacterial microrobots." *J. of Micromechanics and Microengineering*, vol. 21, no. 3, Mar. 2011.

[7] O. Felfoul, M. Mohammadi, L. Gaboury, and S. Martel, "Tumor targeting by computer controlled guidance of magnetotactic bacteria acting like autonomous microrobots," in *IEEE Int. Rob. and Sys.*, 2011, pp. 1304–1308.

[8] Y. Ou, D. H. Kim, P. Kim, M. J. Kim, and A. A. Julius, "Motion control of tetrahymena pyriformis cells with artificial magnetotaxis: Model predictive control (MPC) approach," in *IEEE Int. Conf. Rob. Aut.*, May 2012, pp. 2492–2497.

[9] Y. Shirai, A. J. Osgood, Y. Zhao, K. F. Kelly, and J. M. Tour, "Directional control in thermally driven single-molecule nanocars," *Nano Letters*, vol. 5, no. 11, pp. 2330–2334, Feb. 2005.

[10] P.-T. Chiang, J. Mielke, J. Godoy, J. M. Guerrero, L. B. Alemany, C. J. Villagómez, A. Saywell, L. Grill, and J. M. Tour, "Toward a light-driven motorized nanocar: Synthesis and initial imaging of single molecules," *ACS Nano*, vol. 6, no. 1, pp. 592–597, Feb. 2011.

[11] B. Donald, C. Levey, C. McGray, I. Paprotny, and D. Rus, "An untethered, electrostatic, globally controllable MEMS micro-robot," *J. of MEMS*, vol. 15, no. 1, pp. 1–15, Feb. 2006.

[12] B. Donald, C. Levey, and I. Paprotny, "Planar microassembly by parallel actuation of MEMS microrobots," *J. of MEMS*, vol. 17, no. 4, pp. 789–808, Aug. 2008.

[13] A. Becker and T. Bretl, "Approximate steering of a unicycle under bounded model perturbation using ensemble control," *IEEE Trans. Robot.*, vol. 28, no. 3, pp. 580–591, Jun. 2012.

[14] R. W. Brockett and N. Khaneja, "On the control of quantum ensembles," in *System Theory: Modeling, Analysis and Control*, T. Djaferis and I. Schick, Eds. Kluwer Academic Publishers, 1999.

[15] N. Khaneja, "Geometric control in classical and quantum systems," Ph.D. dissertation, Harvard University, 2000.

[16] J.-S. Li and N. Khaneja, "Ensemble control of Bloch equations," *IEEE Trans. Autom. Control*, vol. 54, no. 3, pp. 528–536, Mar. 2009.

[17] J.-S. Li, "Ensemble control of finite-dimensional time-varying linear systems," *IEEE Trans. Autom. Control*, vol. 56, no. 2, pp. 345–357, Feb. 2011.

[18] P. Lucibello and G. Oriolo, "Robust stabilization via iterative state steering with an application to chained-form systems," *Automatica*, vol. 37, pp. 71–79, 2001.

[19] A. M. Lyapunov, translated and edited by A.T. Fuller, *The General Problem of the Stability of Motion*. London: Tayor & Francis, 1992.

[20] K. Beauchard, J.-M. Coron, and P. Rouchon, "Time-periodic feedback stabilization for an ensemble of half-spin systems," in *IFAC Sym. Nonlin. Cont. Sys.*, Bologna: Italy, Sep. 2010.

[21] J. P. LaSalle, "Some extensions of Liapunov's second method," *IRE Transactions on Circuit Theory*, vol. CT, no. 7, pp. 520–527, Dec. 1960.

[22] W. S. Levine, Ed., *The Control Handbook*. United States of America: CRC Press, Inc., 1996, ch. 25.3 Discrete-Time Linear Time-Varying Systems, pp. 459–463.

[23] S. Thrun, W. Burgard, and D. Fox, *Probabilistic Robotics (Intelligent Robotics and Autonomous Agents)*. The MIT Press, Sep. 2005.

[24] H. Choset, K. Lynch, S. Hutchinson, G. Kantor, W. Burgard, L. Kavraki, and S. Thrun, *Principles of Robot Motion*. The MIT Press, 2005.